

## CO<sub>3</sub><sup>2-</sup>-containing, Dimanganese-Substituted Silicotungstate Trimer,



Ling Yang, Qisen Liu, Pengtao Ma, Jingyang Niu\* and Jingping Wang\*

*Key Laboratory of Polyoxometalates Chemistry of Henan Province, Institute of Molecular and Crystal Engineering, College of Chemistry and Chemical Engineering, Henan University, Kaifeng 475004, China.*

Experimental section.

**Table S1.** The comprehensive literature survey of manganese-substituted silicotungstate derivatives.

**Fig. S1.** Comparison of the simulated and experimental XRPD patterns of the bulk products **1**.

**Fig. S2.** The actual and thumbnail array polyoxoanion structure of **1**.

**Fig. S3.** Visible spectrum of **1**.

**Fig. S4.** The XPS spectra of **1**.

The discussion on the location of protons:

**Fig. S5.** Charge distribution of O atoms in [ $\{\text{SiW}_{10}\text{Mn}^{\text{II}}\text{Mn}^{\text{III}}\text{O}_{38}\}(\text{CO}_3)\text{]}^9-$ .

**Table S2.** The bond valence sum calculations of all the oxygen atoms on POM fragments in **1**.

**Table S3.** The bond valence sum calculations of all the oxygen atoms on polyanion in **1**

**Fig. S6.** Summary of the reported typical trimer polyoxoanion which are similar with **1a**.

**Fig. S7.** IR spectrum for **1** showed the characteristic peaks of carbonate at 1433cm<sup>-1</sup>.

**Fig. S8.** Field dependence of the magnetization of **1**.

**Fig. S9.** The Cyclic voltammograms (CV) of **1** ( $1 \times 10^{-4}$  M) in a pH 6 solution (1 M CH<sub>3</sub>COONa + CH<sub>3</sub>COOH) at a scan rate of 100 mVs<sup>-1</sup>.

**Fig. S10.** The Cyclic voltammograms (CV) of **1** ( $1 \times 10^{-4}$  M) in a pH 6 solution (1 M CH<sub>3</sub>COONa + CH<sub>3</sub>COOH) at different scan rates.

**Fig. S11.** Variation of peak current intensity of the Mn-oxidation peak (a) and W-reduction peak (b) as a function of the square root of the potential scan rate.

**Fig. S12.** The UV curves of **1** in a pH 6 solution (1 M CH<sub>3</sub>COONa + CH<sub>3</sub>COOH) for six hours.

**Fig. S13.** The TG curve of **1**.

## Experimental section

### General methods and materials

The starting materials  $K_6Na_2SiW_{11}O_{39} \cdot 13H_2O$  and  $[Mn_{12}O_2(OMe)_2(thme)_4(OAc)_{10}(H_2O)_4] \cdot 2MeOH$   $\{Mn_{12}\}$  were synthesized according to the literature and confirmed by infrared (IR) spectroscopy. Other chemical reagents were used as commercially purchased and without any further purification. IR spectroscopy was recorded on Nicolet FT-IR 360 spectrometer using KBr pellet in the range 4000-400  $cm^{-1}$ . UV-vis spectra was obtained with a U-4100 spectrometer at room temperature. The power X-ray diffraction (XRPD) measurement was performed on a Philips X'Pert-MPD instrument with Cu  $K\alpha$  radiation ( $\lambda = 1.54056 \text{ \AA}$ ) in the range  $2\theta = 10\text{--}40^\circ$  at 293 K. TG analysis was performed under  $N_2$  atmosphere on a Mettler-Toledo TGA / SDTA851<sup>e</sup> instrument with a heating rate of  $10^\circ C/min^{-1}$  from 25 to  $600^\circ C$ . X-ray photoelectron spectroscopy (XPS) was performed on an Axis Ultra (Kratos, U.K.) photoelectron spectroscope using monochromatic Al  $K\alpha$  (1486.7 eV) radiation. Magnetic measurement was carried out on Quantum Design MPMS SQUID VSM magnetometer in the temperature range 2-300 K at 1000 Oe. Elemental analyse (C, H and N) was conducted on a Perkin-Elmer 2400-II CHNS/O Analyzer. Inductively coupled plasma atomic emission spectrometry (ICP-AES) analyse was conducted on a Perkin-Elmer Optima 2000 ICP-OES spectrometer.

### Synthesis

**$K_9[H_{14}\{SiW_{10}Mn^{II}Mn^{III}O_{38}\}_3(CO_3)] \cdot 39H_2O$  (1):**  $\{Mn_{12}\}$  (0.502g, 0.26mmol) was dissolved in 20ml ethanol and stirred until complete dissolution resulting in solution A.  $K_6Na_2SiW_{11}O_{39} \cdot 13H_2O$  (1.00g, 0.31mmol) was dissolved in 20 mL distilled water resulting in solution B. After clarification, the pH of the solution B was adjusted to ca. 10.0 with  $2.0 \text{ mol L}^{-1}$   $K_2CO_3$  under stirring. Then, 1.2ml solution A was added. The resulting turbid mixture was stirred approximately 5h at  $80^\circ C$  after stirring more than 3 h at room temperature. After cooling down to ambient temperature, the precipitate was filtered off. The deep-brown block crystals of **1** were obtained by slow evaporation at room temperature after three days. Yield: ca. 0.033g (24% based on  $\{Mn_{12}\}$ ). Anal. Calcd. (%) for **(1)**: C, 0.14; H, 1.04; K, 3.96; Mn, 3.71; W, 62.10; Si, 0.95; found: C, 0.14; H, 1.07; **K, 4.05; Mn, 3.95; W, 61.70; Si, 1.02**; IR (KBr pellet): 3468, 1628, 1433, 993, 943, 896, 778, 718, and  $535 \text{ cm}^{-1}$ .

### X-ray crystallography.

Suitable single crystal was selected from the mother liquors and stucked on the end of a glass rod. Intensity data for **1** was collected on Bruker Apex-II CCD diffractometer with the graphite-monochromated Mo  $K\alpha$  radiation ( $\lambda = 0.71073 \text{ \AA}$ ) at 296(2) K. Routine Lorentz polarization and empirical absorption corrections were applied. The structure was solved by the direct methods and refined by the full-matrix least-squares method on  $F^2$  with the SHELXTL-97 program package.<sup>1</sup> No hydrogen atoms associated with the water molecules were located from the difference Fourier map. All hydrogen atoms were refined isotropically as a riding mode using the default SHELXTL parameters. In **1**, the six positions of W6 are simultaneously statistically occupied by Mn2 and W6 elements with half occupancy for each. Further details of the crystal structure investigation may be obtained from Fachinformationszentrum Karlsruhe, 76344 Eggenatein-Leopoldshafen, Germany (fax: (+49)7247-808-666; e-mail: crystdata@fiz-karlsruhe.de) on quoting the depository numbers CSD-429047.

[1] (a) G. M. Sheldrick, SHELXL 97, Program for Crystal Structure Refinement; University of Göttingen, Germany, 1997; (b) G. M. Sheldrick, SHELXS 97, Program for Crystal Structure Solution; University of Göttingen: Göttingen, Germany, 1997.

**Synthetic discussion.** From the synthetic point of view, Mn<sup>III</sup>-substituted POMs can be prepared by means of the following ways: the first way is to use prepared POM precursor interaction with a simple Mn<sup>II</sup> salt (e. g. chloride or perchlorate) under the condition of a higher pH, since the Mn<sup>2+</sup> could be oxidized to Mn<sup>3+</sup> ions by oxygen under alkaline conditions, or add the strong oxidation agents (e. g. KMnO<sub>4</sub>) in reaction system so as to transform Mn<sup>II</sup> into Mn<sup>III</sup>.<sup>2</sup> Another better alternative synthetic route is to replace simple Mn<sup>II</sup> salt with preformed Mn complexes (e.g. [Mn<sup>III</sup><sub>8</sub>Mn<sup>IV</sup><sub>4</sub>O<sub>12</sub>(CH<sub>3</sub>COO)<sub>16</sub>(H<sub>2</sub>O)<sub>4</sub>]·4H<sub>2</sub>O·2CH<sub>3</sub>COOH (Mn<sub>12</sub>-acetate), [Mn<sub>2</sub>(5-MeOsaltmen)<sub>2</sub>(H<sub>2</sub>O)<sub>2</sub>](PF<sub>6</sub>)<sub>2</sub>, [Mn<sub>2</sub>(salen)<sub>2</sub>(H<sub>2</sub>O)<sub>2</sub>](ClO<sub>4</sub>)<sub>2</sub> and [Mn<sub>2</sub>(5-Brsaltmen)<sub>2</sub>(H<sub>2</sub>O)<sub>2</sub>](PF<sub>6</sub>)<sub>2</sub>) to react with various POM ligands.<sup>3</sup> Moreover, with the knowledge of the precursor [SiW<sub>11</sub>O<sub>39</sub>]<sup>8-</sup> may slowly rearrange to [SiW<sub>12</sub>O<sub>40</sub>]<sup>4-</sup> or combine with a manganese ions to [SiW<sub>11</sub>MnO<sub>40</sub>]<sup>n-</sup> in suitable acidity system in mind, we make the reaction process taken place in alkaline condition. Herein, we replace the commonly used Mn<sub>12</sub>-acetate, which was synthesized in acidic system, with {Mn<sub>12</sub>}, which was isolated from the alkaline environment. It is worth pointing out when {Mn<sub>12</sub>} was replaced by MnCl<sub>2</sub>·4H<sub>2</sub>O, the replacement of [SiW<sub>11</sub>O<sub>39</sub>]<sup>8-</sup> with [GeW<sub>11</sub>O<sub>39</sub>]<sup>8-</sup>, or using alternative anions such as [α-SiW<sub>9</sub>O<sub>34</sub>]<sup>10-</sup> or [γ-SiW<sub>10</sub>O<sub>36</sub>]<sup>8-</sup>, **1** or its analogues could not be obtained under the similar conditions, indicating that both {Mn<sub>12</sub>} complexes and [SiW<sub>11</sub>O<sub>39</sub>]<sup>8-</sup> precursor play an important role.

[2] (a) D. Shevchenko, P. Huang, V. V. Bon, M. F. Anderlund, V. N. Kokozay, S. Styring and A. Thapper, *Dalton Trans.*, 2013, **42**, 5130; (b) J. Thiel, P. I. Molina, M. D. Symes and L. Cronin, *Cryst. Growth Des.*, 2012, **12**, 902.

[3] (a) X. K. Fang, P. Kögerler, M. Speldrich, H. Schilder and M. Luban, *Chem. Commun.*, 2012, **48**, 1218; (b) Y. K. Sawada, W. Kosaka, Y. Hayashi and H. Miyasaka, *Inorg. Chem.*, 2012, **51**, 4824; (c) Yuki Sawada, Wataru Kosaka, Yoshihito Hayashi, and Hitoshi Miyasaka, *Inorg. Chem.*, 2012, **51**, 4824.

**Table S1.** The comprehensive literature survey of manganese-substituted silicotungstate derivatives.

Formula	M n	POM precursor	Year	Re f
$[\text{Mn}^{\text{II}}(\text{H}_2\text{O})_2(\gamma\text{-SiW}_{10}\text{O}_{35})_2]^{10-}$	1	$\text{K}_8[\gamma\text{-SiW}_{10}\text{O}_{36}] \cdot 12\text{H}_2\text{O}$	2006	1
$[(\text{CH}_3)_3(\text{C}_6\text{H}_5)\text{N}]_4[(\text{SiO}_4)\text{W}_{10}\text{Mn}^{\text{III}}_2\text{O}_{36}\text{H}_6] \cdot 2\text{CH}_3\text{CN} \cdot \text{H}_2\text{O}$	2	$\text{K}_8[\gamma\text{-SiW}_{10}\text{O}_{36}] \cdot 12\text{H}_2\text{O}$	1996	2
$[\text{Mn}_2(5\text{-MeOsaltmen})_2(\text{acetone})_2][\text{SiW}_{12}\text{O}_{40}]$	2/ 4	$(n\text{-Bu}_4\text{N})_2[\text{SiW}_{12}\text{O}_{40}]$	2012	3
$[\text{Mn}_2(\text{salen})_2(\text{H}_2\text{O})_2][\text{SiW}_{12}\text{O}_{40}]$				
$[\text{Mn}(5\text{-Brsaltmen})(\text{H}_2\text{O})(\text{acetone})]_2[\{\text{Mn}_2(5\text{-Brsaltmen})_2\}(\text{SiW}_{12}\text{O}_{40})]$				
$[\text{Mn}^{\text{II}}\text{Mn}^{\text{III}}(\text{OH})(\text{H}_2\text{O})\text{SiW}_{10}\text{O}_{37}]^{6-}$	2	$\text{Na}_{10}[\alpha\text{-SiW}_9\text{O}_{34}] \cdot 15\text{H}_2\text{O}$	2013	4
$[\text{Mn}^{\text{II}}_3(\text{H}_2\text{O})_3\text{SiW}_9\text{O}_{37}]^{10-}$	3	$\beta\text{-Na}_9\text{H}[\text{SiW}_9\text{O}_{34}] \cdot 23\text{H}_2\text{O}$	1992	5
$[(\beta_2\text{-SiW}_{11}\text{MnO}_{38}\text{OH})_3]^{15-}$	3	$\text{K}_8[\gamma\text{-SiW}_{10}\text{O}_{36}] \cdot 12\text{H}_2\text{O}$	2001	6
$[\text{Mn}^{\text{III}}_3(\text{OH})_3(\text{H}_2\text{O})_3\text{SiW}_9\text{O}_{34}]^{4-}$	3	$\text{K}_8[\gamma\text{-SiW}_{10}\text{O}_{36}] \cdot 12\text{H}_2\text{O}$	2013	7
$[\text{Mn}^{\text{II}}_3(\text{OH})_3(\text{H}_2\text{O})_3(\text{A-}\alpha\text{-SiW}_9\text{O}_{34})]^{7-}$ , $[\text{Mn}^{\text{III}}_3(\text{OH})_3(\text{H}_2\text{O})_3(\text{A-}\alpha\text{-SiW}_9\text{O}_{34})]^{4-}$	3	$\text{K}_{10}[\text{A-}\alpha\text{-SiW}_9\text{O}_{34}] \cdot 24\text{H}_2\text{O}$	2014	8
$[\text{Mn}^{\text{III}}_3(\text{OH})_3(\text{H}_2\text{O})_3(\text{A-}\beta\text{-SiW}_9\text{O}_{34})]^{4-}$ , $[\text{Mn}^{\text{III}}_3\text{Mn}^{\text{IV}}\text{O}_3(\text{CH}_3\text{COO})_3(\text{A-}\beta\text{-SiW}_9\text{O}_{34})]^{6-}$	3/ 4	$\text{Na}_9[\text{A-}\beta\text{-SiW}_9\text{O}_{34}\text{H}] \cdot 23\text{H}_2\text{O}$		
$[\text{Mn}^{\text{III}}_3\text{Mn}^{\text{IV}}\text{O}_3(\text{CH}_3\text{COO})_3(\text{A-}\alpha\text{-SiW}_9\text{O}_{34})]^{6-}$ ,	4	$\text{Na}_{10}[\text{A-}\alpha\text{-SiW}_9\text{O}_{34}] \cdot 14\text{H}_2\text{O}$		
$[\{\text{SiMn}_2\text{W}_9\text{O}_{34}(\text{H}_2\text{O})_2\}]^{12-}$	4	$\text{K}_8[\gamma\text{-SiW}_{10}\text{O}_{36}] \cdot 12\text{H}_2\text{O}$	2000	9
$[\{\text{Mn}^{\text{II}}_2(\text{SiW}_{10}\text{O}_{36})(\text{OH})_2(\text{N}_3)_{0.5}(\text{H}_2\text{O})_{0.5}\}_2(\text{N}_3)]^{10-}$	4	$[\text{N}(\text{C}_4\text{H}_9)_4]_4\text{H}_4[\gamma\text{-SiW}_{10}\text{O}_{36}]$	2006	10
$[\{\text{Dy}^{\text{III}}\text{Mn}^{\text{III}}_4(\mu_3\text{-O})_2(\mu_2\text{-OH})_2(\text{H}_2\text{O})(\text{CO}_3)\}(\beta\text{-SiW}_8\text{O}_{31})_2]^{13-}$	4	$\text{K}_8[\gamma\text{-SiW}_{10}\text{O}_{36}] \cdot 12\text{H}_2\text{O}$	2013	11
$[\{\text{SiW}_9\text{O}_{34}\}_2[\text{Mn}^{\text{III}}_4\text{Mn}^{\text{II}}_2\text{O}_4(\text{H}_2\text{O})_4]_2]^{12-}$	6	$\text{K}_8[\gamma\text{-SiW}_{10}\text{O}_{36}] \cdot 12\text{H}_2\text{O}$	2008	12
$[\text{Mn}^{\text{III}}_2\text{Mn}^{\text{II}}_4\text{O}_2(\text{H}_2\text{O})_4(\text{SiW}_8\text{O}_{31})(\text{SiW}_9\text{O}_{34})(\text{SiW}_{10}\text{O}_{36})]^{18-}$	6	$\text{K}_8[\gamma\text{-SiW}_{10}\text{O}_{36}] \cdot 12\text{H}_2\text{O}$	2011	13
$\{\{\text{Mn}(\text{H}_2\text{O})_3\}_2[\text{Mn}(\text{H}_2\text{O})_2][(\text{B-}\beta\text{-SiW}_9\text{O}_{33}(\text{OH}))\text{Mn}_3(\text{H}_2\text{O})(\text{B-}\beta\text{-SiW}_8\text{O}_{30}(\text{OH}))_2]\}^{18-}$	9	$\text{K}_8[\gamma\text{-SiW}_{10}\text{O}_{36}] \cdot 12\text{H}_2\text{O}$	2011	14
$\text{K}_{18}[\text{Mn}^{\text{II}}_2\{\text{Mn}^{\text{II}}(\text{H}_2\text{O})_5\text{Mn}^{\text{III}}_3(\text{H}_2\text{O})(\text{B-}\beta\text{-SiW}_9\text{O}_{34})(\text{B-}\beta\text{-SiW}_6\text{O}_{26})\}_2] \cdot 20\text{H}_2\text{O}$	10	$\text{K}_8[\gamma\text{-SiW}_{10}\text{O}_{36}] \cdot 12\text{H}_2\text{O}$	2010	15
$(\text{C}_4\text{H}_{10}\text{NO})_{40}[\text{W}_{72}\text{Mn}^{\text{III}}_{12}\text{X}_7\text{O}_{268}] \cdot 48\text{H}_2\text{O}$ (X = Si or Ge)	12	$\text{K}_8[\gamma\text{-SiW}_{10}\text{O}_{36}] \cdot 12\text{H}_2\text{O}$	2012	16
$\{\{\text{Mn}^{\text{IV}}_2\text{Mn}^{\text{III}}_6\text{Mn}^{\text{II}}_4(\mu_3\text{-O})_6(\mu\text{-OH})_4(\text{H}_2\text{O})_2(\text{CO}_3)_6\}[\text{B-}\beta\text{-SiW}_6\text{O}_{26}]_2\}^{18-}$	12	$\text{K}_8[\beta_2\text{-SiW}_{11}\text{O}_{39}]$	2013	17
$[\text{Mn}^{\text{II}}_{19}(\text{OH})_{12}(\text{SiW}_{10}\text{O}_{37})_6]^{34-}$	19	$\text{Na}_{10}[\text{A-}\alpha\text{-SiW}_9\text{O}_{34}] \cdot 14\text{H}_2\text{O}$	2011	18

## Reference

- [1] B. S. Bassil, M. H. Dickman, M. Reicke, U. Kortz, B. Keita and L. Nadjo, *Dalton Trans.*, 2006, 4253.
- [2] X. Y. Zhang, C. J. O'Connor, G. B. Jameson and M. T. Pope, *Inorg. Chem.*, 1996, **35**, 30.
- [3] Y. K. Sawada, W. Kosaka, Y. Hayashi and H. Miyasaka, *Inorg. Chem.*, 2012, **51**, 4824.
- [4] P. Emmanuel Car, B. Spingler, S. Weyeneth, J. Patscheider and G. R. Patzke, *Polyhedron.*, 2013, **52**, 151.
- [5] J. F. Liu, F. Ortéga, P. Sethuraman, D. E. Katsoulis, C. E. Costello and M. T. Pope, *J. Chem. Soc., Dalton Trans.*, 1992, 1901.
- [6] U. Kortz and S. Matta, *Inorg. Chem.*, 2001, **40**, 815.
- [7] D. Shevchenko, P. Huang, V. V. Bon, M. F. Anderlund, V. N. Kokozay, S. Styring and Anders Thapper, *Dalton Trans.*, 2013, **42**, 5130.
- [8] R. Al-Oweini, B. S. Bassil, J. Friedl, V. Kottisch, M. Ibrahim, M. Asano, B. Keita, G. Novitchi, Y. H. Lan, A. Powell, U. Stimming and U. Kortz, *Inorg. Chem.*, 2014, **53**, 5663.

- [9] U. Kortz, S. Isber, M. H. Dickman and D. Ravot, *Inorg. Chem.*, 2000, **39**, 2915.
- [10] P. Mialane, C. Duboc, J. Marrot, E. Rivière, A. Dolbecq and F. Sécheresse, *Chem. Eur. J.*, 2006, **12**, 1950.
- [11] H. H. Wu, S. Yao, Z. M. Zhang, Y. G. Li, Y. Song, Z. J. Liu, X. B. Han and E. B. Wang, *Dalton Trans.*, 2013, **42**, 342.
- [12] C. Ritchie, A. Ferguson, H. Nojiri, H. N. Miras, Y. F. Song, D. L. Long, E. Burkholder, M. Murrie, P. Kögerler, E. K. Brechin and L. Cronin, *Angew. Chem. Int. Ed.*, 2008, **47**, 5609.
- [13] S. G. Mitchell, P. I. Molina, S. Khanra, H. N. Miras, A. Prescimone, G. J. T. Cooper, R. S. Winter, E. K. Brechin, D. L. Long, R. J. Cogdell and L. Cronin, *Angew. Chem. Int. Ed.*, 2011, **50**, 9154.
- [14] L. J. Chen, D. Y. Shi, J. W. Zhao, Y. L. Wang, P. T. Ma, J. P. Wang and J. Y. Niu, *Cryst. Growth Des.*, 2011, **11**, 1913.
- [15] S. G. Mitchell, H. N. Miras, D. L. Long and L. Cronin, *Inorganica Chimica Acta.*, 2010, **363**, 4240.
- [16] J. Thiel, P. I. Molina, M. D. Symes and L. Cronin, *Cryst. Growth Des.*, 2012, **12**, 902.
- [17] Z. M. Zhang, S. Yao, Y. G. Li, H. H. Wu, Y. H. Wang, M. Rouzières, R. Clérac, Z. M. Su and E. B. Wang, *Chem. Commun.*, 2013, **49**, 2515.
- [18] B. S. Bassil, M. Ibrahim, R. Al-Oweini, M. Asano, Z. X. Wang, J. Van Tol, N. S. Dalal, K. Yong Choi, R. N. Biboum, B. Keita, L. Nadjo and U. Kortz, *Angew. Chem. Int. Ed.*, 2011, **50**, 5961.

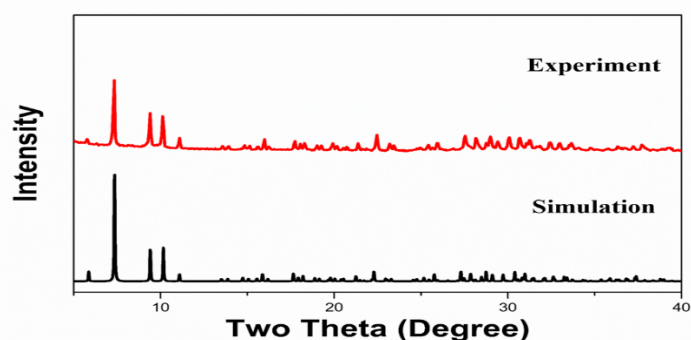


**Fig. S1.** Comparison of the simulated and experimental XRPD patterns of the bulk products **1**.

The experimental XRPD pattern for **1** is in good agreement with the simulated XRPD pattern from the single-crystal X-ray diffraction, demonstrating good phase purity for **1**.

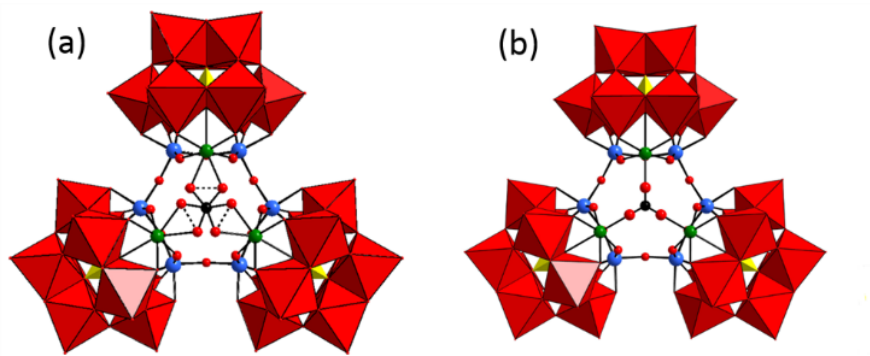


**Fig. S2.** (a) The actual polyoxoanion structure of **1** on the crystallography. (b) The thumbnail array of **1a**. Because of O atoms around C atom are disordered, we present **1a** with figure b briefly, so that we can be easily understand.

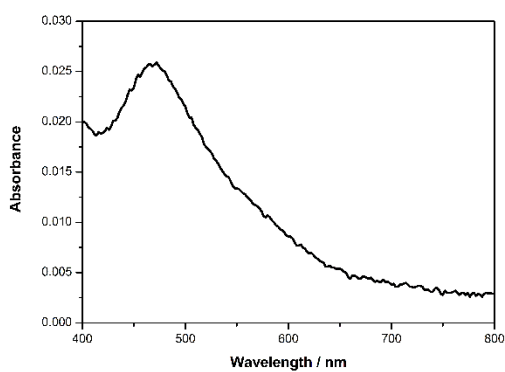


**Fig. S3.** Visible spectrum of **1**.

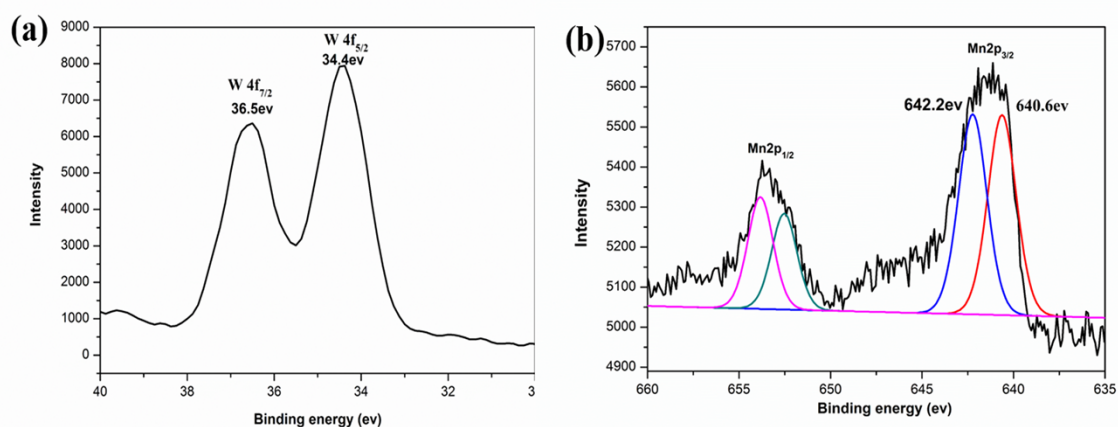


**Fig. S4.** (a) XPS spectra of **1** for W  $4f_{5/2}$  and W  $4f_{7/2}$ ; (b) XPS spectra of **1** for Mn  $2p_{1/2}$  and Mn  $2p_{3/2}$

The bond-valence sum ( $\Sigma_s$ ) calculations show that all Mn1 and W in **1** are in the +3 and +6 oxidation states, respectively. According to the charge balances, fourteen protons should be added for charge balance. These protons are difficult to be located crystallographically and it has been hypothesized that they are delocalized over the entire structures, This phenomenon is very common in POM chemistry, for example,  $[\text{Sn}_4(\text{SiW}_9\text{O}_{34})_2]^{12-}$ ,<sup>1</sup>  $[\text{H}_{23}\text{NaO}_8\text{Cu}_{24}(\text{Nb}_7\text{O}_{22})_8]^{16-}$  and  $[\text{H}_9\text{Cu}_{25.5}\text{O}_8(\text{Nb}_7\text{O}_{22})_8]^{28-}$ ,<sup>2</sup>  $[\text{HW}_9\text{O}_{33}\text{Ru}^{\text{II}}_2(\text{dmsO})_6]^{7-}$ ,<sup>3</sup>  $[\text{H}_3\text{W}_{12}\text{O}_{40}]^{5-}$ ,<sup>4</sup> Considering the POM fragments  $[\{\text{SiW}_{10}\text{Mn}^{\text{II}}\text{Mn}^{\text{III}}\text{O}_{38}\}_3(\text{CO}_3)]^{23-}$  units possess the high negative charges and the oxygen-enriched surfaces, so we reasoned that the POM fragments are easily protonated. In **1**, except for the 30 O atoms which bond to the disordered Mn2/W, the rest of 87 O atoms can be divided into four groups according to the BVS. The results as follows: there are 24 O atoms with their  $\Sigma_s$  in the range of  $-2.01 \sim -2.08$ , and 24 O atoms with their  $\Sigma_s$  in the range of  $-1.91 \sim -1.98$ , and 33 O atoms with their  $\Sigma_s$  in the range of  $-1.72 \sim -1.83$ , and 6 O atoms with their  $\Sigma_s$  are 1.56. So there are great opportunities for the fourteen protons to be delocalized on these O atoms, especially the 6 O atoms with their  $\Sigma_s$  are 1.56 and the 33 O atoms with their  $\Sigma_s$  in the range of  $-1.72 \sim -1.83$ .

- [1] Z. Y. Zhang, Q. P. Lin, S. T. Zheng, X. H. Bu and P. Y. Feng, *Chem. Commun.*, 2011, **47**, 3918.  
 [2] J. Y. Niu, P. T. Ma, H. Y. Niu, J. Li, J. W. Zhao, Y. Song and J. P. Wang, *Chem. Eur. J.*, 2007, **13**, 8739.  
 [3] L. Bi, F. Hussain, U. Kortz, M. Sadakane and M. H. Dickman, *Chem. Commun.*, 2004, **12**, 1420.  
 [4] C. Streb, C. Ritchie, D. L. Long, P. Kögerler and L. Cronin, *Angew. Chem.*, 2007, **119**, 7723, *Angew. Chem. Int. Ed.*, 2007, **46**, 7579.

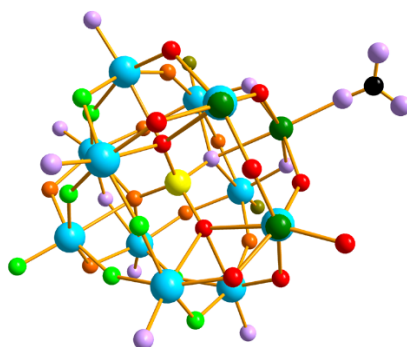


**Fig. S5.** Charge distribution of O atoms in  $[\{\text{SiW}_{10}\text{Mn}^{\text{II}}\text{Mn}^{\text{III}}\text{O}_{38}\}_3(\text{CO}_3)]^{9-}$ . The O atoms with different colors are separated on the basis of the different bond valence sums.

**Table S2.** The bond valence sum calculations of all the oxygen atoms on POM fragments in **1**.

Oxygen	Band valence sum range	Number	Oxygen	Band valence sum range	Number
	–	30		–1.72 ~ –1.83	33
	–2.01 ~ –2.08	24		1.56	6
	–1.91 ~ –1.98	24			

**Table S3.** The bond valence sum calculations of all the oxygen atoms on polyanion in **1**.

Atom	Bond valence sum	Atom	Bond valence sum	Atom	Bond valence sum
O1	2.03	O7	1.94	O13	1.95
O2	1.97	O8	2.06	O14	1.77
O3	2.08	O9	1.56	O15	2.05
O4	1.92	O10	1.94	O16	2.08
O5	1.76	O11	1.82	O19	1.73
O6	1.83	O12	1.79	O24	1.76

O17, O18, O20, O21, O22 and O23 are bond to the disordered Mn/W.

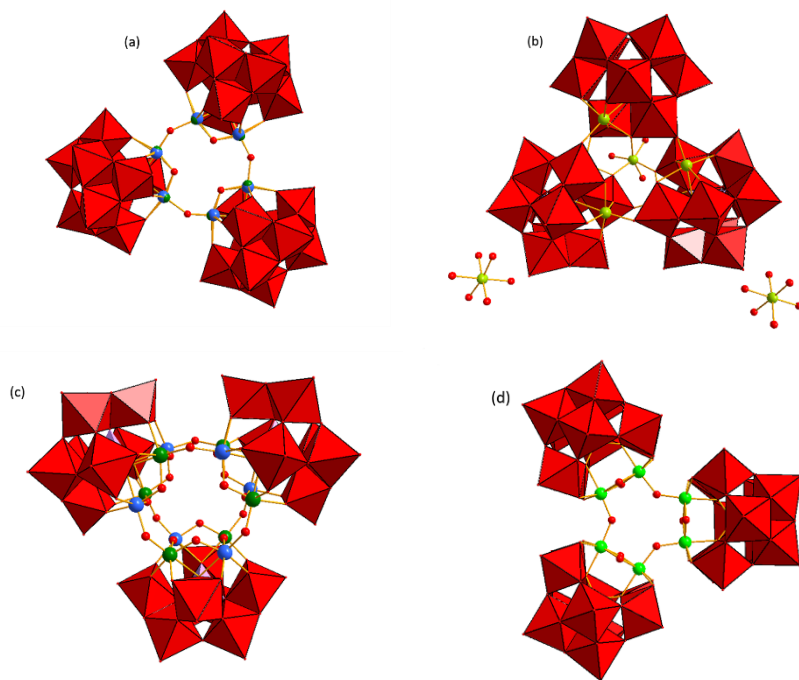


**Fig. S6.** Summary of the reported typical trimer polyoxoanion which are similar with **1a**. (a)  $[(\beta_2\text{-SiW}_{11}\text{MnO}_{38}\text{OH})_3]^{15-}$ ; (b)  $[\text{Co}(\text{H}_2\text{O})_6]_2[\text{Co}(\text{H}_2\text{O})_3(\alpha\text{-GeW}_{11}\text{CoO}_{38})_3]^{6-}$ ; (c)  $[(\text{Mn}^{\text{II}}_2\text{GeW}_{10}\text{O}_{38})_3]^{18-}$ ; (d)  $[\{\gamma\text{-H}_2\text{SiW}_{10}\text{O}_{36}\text{Al}_2(\mu\text{-OH})_2(\mu\text{-OH})\}_3]^{9-}$ . In a, b and c, both of the M and W locating in the metal cluster are disordered. This phenomenon is also happened on **1a**.

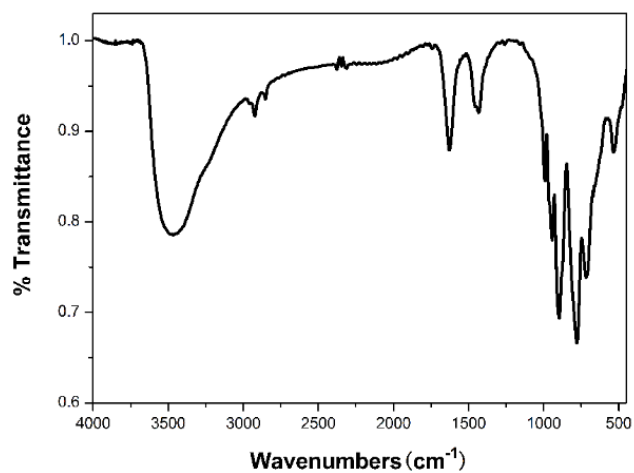


**Fig. S7.** IR spectrum for **1** showed the characteristic peaks of carbonate at  $1433\text{cm}^{-1}$ .

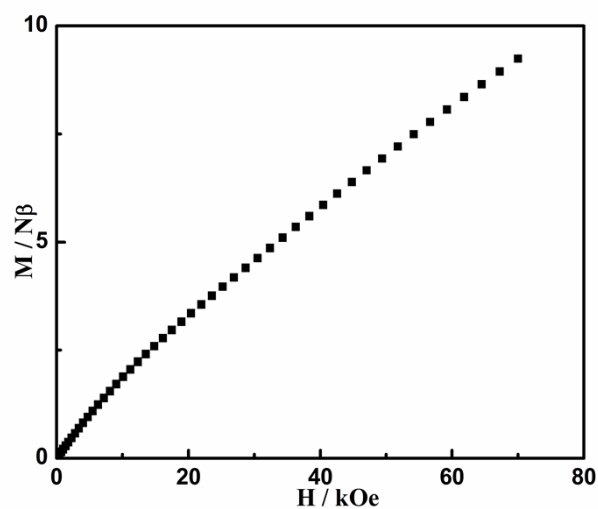


**Fig. S8.** Field dependence of the magnetization of **1**.

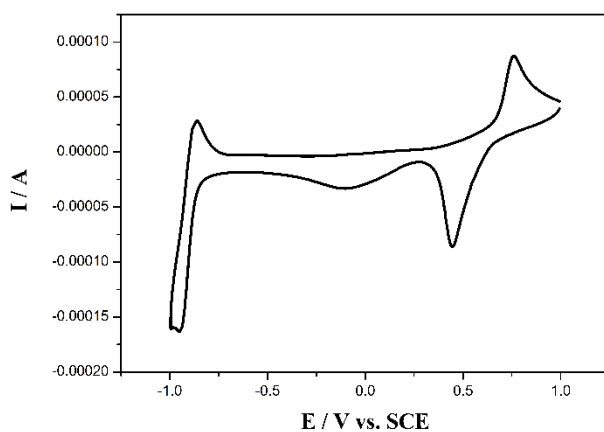


**Fig. S9.** Cyclic voltammograms (CV) of  $1 \times 10^{-4}$  M **1** in a pH 6 medium (1 M  $\text{CH}_3\text{COONa}$  +  $\text{CH}_3\text{COOH}$ ) at a scan rate of  $100 \text{ mVs}^{-1}$  with the initial sweep towards the negative region of potential values. The working electrode was pretreated indium tin oxide (ITO) electrode and the reference electrode was saturated calomel reference electrode (SCE).

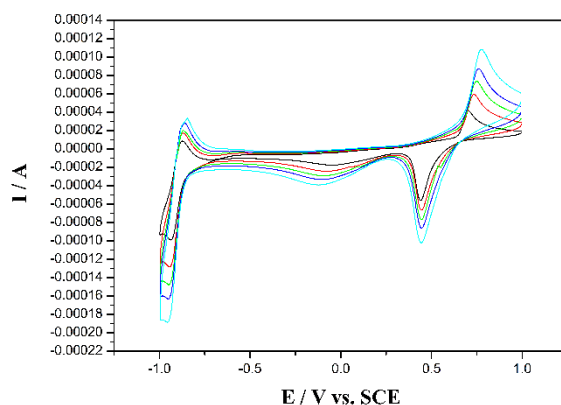


**Fig. S10.** The Cyclic voltammograms (CV) of **1** ( $1 \times 10^{-4}$  M) in a pH 6 solution (1 M  $\text{CH}_3\text{COONa} + \text{CH}_3\text{COOH}$ ) at different scan rates.

Cyclic voltammograms (CV) of  $1 \times 10^{-4}$  M **1** in a pH 6 medium (1 M  $\text{CH}_3\text{COONa} + \text{CH}_3\text{COOH}$ ) at scan rates (from inner to outer) of 25, 50, 75, 100 and 150  $\text{mVs}^{-1}$  with the initial sweep towards the negative region of potential values. The working electrode was a pretreated indium tin oxide (ITO) electrode. Potentials were measured against a saturated calomel reference electrode (SCE). The counter electrode was a platinum electrode. The solutions was deaerated thoroughly for 30 min with pure argon and kept under a positive pressure of this gas during the experiments.

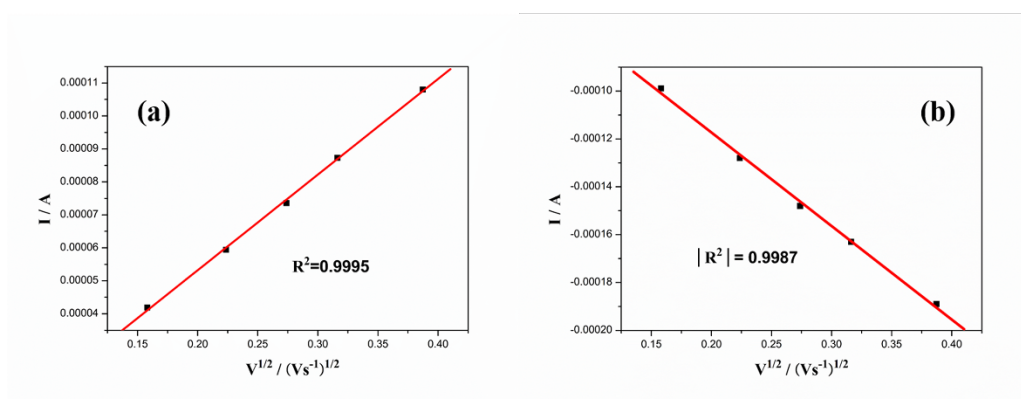


**Fig. S11.** Variation of peak current intensity of the Mn-oxidation peak (a) and W-reduction peak (b) as a function of the square root of the potential scan rate. The linearity are 0.9995 and 0.9987, respectively.

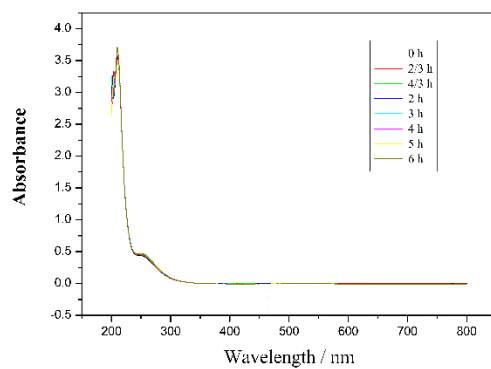


**Fig. S12.** The UV-vis curves of **1** in a pH 6 solution (1 M CH<sub>3</sub>COONa + CH<sub>3</sub>COOH) for six hours.

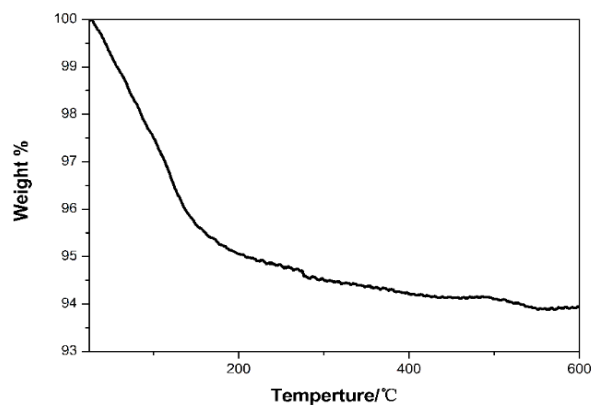


**Fig. S13.** The TG curve of **1**.